Noname manuscript No.
(will be inserted by the editor)

Gait generation for a biped robot with knees and torso via trajectory learning and state-transition estimation

Satoshi Satoh · Kenji Fujimoto

Received: date / Accepted: date

Abstract The proposed method can generate an optimal feedforward control input and the corresponding optimal walking trajectory minimizing the L_2 norm of the control input by iteration of laboratory experiments. Since a general walking motion involves discontinuous velocity transitions caused by the collision with the ground, the proposed method consists of the combination of a trajectory learning part and an estimation part of the discontinuous state transition mapping by using the stored experimental data. We apply the proposed method to a kneed biped robot with a torso, where we also provide a technique to generate an optimal gait not only being energy-efficient but also avoiding the foot-scuffing problem.

1 Introduction

So far, controlling walking robots has attracted much research interest. Particularly, walking pattern generation is a fundamental and important subject in this research area. As various methods have been proposed, pattern generation methods are evolving from assigning a heuristic walking pattern to generating an optimal one. Therefore, the optimization of walking gaits with respect to the energy consumption becomes increasingly important. In order to generate an energy efficient walking pattern, the passive dynamic walker [15] also attracts attention [16, 17, 12, 13]. This robot has a certain simple structure without actuators and it walks down on a gentle slope. The uncontrolled dynamics of the passive walker intrinsically possesses a stable limit cycle. Walking control methods based on the passive dynamic walking have been proposed by many researchers, e.g. [9, 23, 11, 2, 1, 24]. Although the generated gaits are energy efficient, these methods are only applicable to certain specially structured robots so far.

On the contrary, we have developed a model-free optimal gait generation framework by using a universal property of mechanical systems and learning control [18–21]. Our method is based on the iterative learning control (ILC) proposed in [8], which utilizes a property of Hamiltonian systems called variational symmetry. A Hamiltonian system is one of the representations of a physical system, and thus many kinds of walking robots can be uniformly described as Hamiltonian systems. Our technique can generate an optimal periodic gait which minimizes a cost function by iteration of laboratory experiments. The cost function mainly consists of two terms: one attempts to minimize the L_2 norm of the control input, and the other attempts to make a trajectory periodic, which is a constraint term for a periodic gait. By taking advantage of the variational symmetry of Hamiltonian systems, the proposed method does not require the precise model of the plant system. So far, in numerical simulations, we have generated an optimal running gait of a planer one-legged hopping robot [18] and optimal walking gaits of a planer compass-like biped robot [19, 21] and one with a torso [20], respectively.

This work was partially supported by JSPS KAKENHI Grant Numbers JP17H03282 and JP18K04202.

S. Satoh
Osaka University, 2-1, Yamadaoka, Suita, Osaka 565-0871, Japan
E-mail: s.satoh@ieee.org

K. Fujimoto
Kyoto University, Yoshida-Honmachi, Sakyo-ku, Kyoto 606-8501, Japan
E-mail: fujimoto@kuaero.kyoto-u.ac.jp

In this paper, we consider a kneed biped robot with a torso, and propose a modification of our previous learning gait generation methods in properly considering discontinuous velocity transitions. Since a general walking motion involves discontinuous velocity transitions caused by the collision with the ground, the proposed method not only executes trajectory learning, but also estimates a mapping of such transitions with the stored experimental data. The significance of introducing knees for the compass-like bipeds are as follows. First, we can investigate more general and human-like walking motions. Second, controlling knees enables a walking robot to achieve a proper foot clearance, and to avoid the foot scuffing problem [15,10], which is an unavoidable issue of compass-like bipeds. The foot scuffing problem is that the swing leg scuffs the ground when it passes the stance leg, and this phenomenon causes the robot to fall down. Regarding this, in this paper, we also provide a technique for kneed bipeds to avoid this problem. We deal with a necessary condition for a periodic trajectory that the state just after the collision between the swing leg and the ground coincides with the initial state as a state constraint. Here, the state consists of the joint angle and angular velocity of the robot. In order to achieve this state constraint, our previous works [19,21] assigned the desired terminal angle and velocity with the joint angle and angular velocity separately. However, the conflict between the desired angle and velocity occasionally happens in learning, and then the both conditions cannot be achieved simultaneously. To overcome this problem, the proposed method newly equip a reference trajectory such that the terminal constraints of the angle and velocity are simultaneously satisfied. Although calculation of such reference trajectory generally requires information of the state transition mapping which maps from the velocity just before the collision to that just after the transition, the proposed method considers it to be an unknown nonlinear function, and estimates its Jacobian by the recursive least-squares with the stored experimental data. Consequently, the proposed method generates an optimal periodic gait, which is energy-efficient, and also avoids the foot-scuffing problem without the precise models of the plant system nor the state transition mapping. The present paper provides more efficient estimation scheme of the state transition mapping than an early version in [22], where the pseudo inverse matrix is employed. Finally, numerical simulations demonstrate the effectiveness of the proposed method.

2 Preliminaries

This section briefly refers to preliminary backgrounds.

2.1 Hamiltonian systems and variational symmetry

We consider a Hamiltonian system [4,14] with a controlled Hamiltonian $H(x,u)$ denoted by $\Sigma^{x_{t^0}} : U \to Y : u \mapsto y$ as

$$\Sigma^{x_{t^0}} : \begin{cases} \dot{x} = (J - R)\dfrac{\partial H(x,u)}{\partial x}^{\top}, \quad x(t^0) = x_{t^0} \\ y = -\dfrac{\partial H(x,u)}{\partial u}^{\top} \end{cases} . \tag{1}$$

This representation includes typical mechanical systems, and thus many kinds of walking robots can be uniformly described as the form (1). Here, $x(t) \in X$, $u \in U$ and $y \in Y$ with Hilbert spaces, and they describe the state, the input and the output, respectively. Typically, $X = \mathbb{R}^n$ and $U, Y = L_2^m[t^0, t^1]$ on a finite time interval $[t^0, t^1]$. The structure matrix $J \in \mathbb{R}^{n\times n}$ and the dissipation matrix $R \in \mathbb{R}^{n\times n}$ are skew-symmetric and symmetric positive semi-definite, respectively.

The variational system denoted by $\delta\Sigma^{x_{t^0}}$ is derived from the Fréchet derivative of the system $\Sigma^{x_{t^0}}$. Since we consider $\Sigma^{x_{t^0}}$ to be an operator on $L_2^m[t^0, t^1]$, the adjoint system of the variational one denoted by $(\delta\Sigma^{x_{t^0}})^*$ is also considered. Both systems later appear and play an important role in the gradient calculation of the cost function for derivation of the iteration law. The literature [8] clarified a special property between the state-space realizations of $\delta\Sigma^{x_{t^0}}$ and $(\delta\Sigma^{x_{t^0}})^*$, which is called the variational symmetry of Hamiltonian systems. In short, the variational symmetry implies that under some conditions, a state-space realization of the adjoint system with zero terminal state coincides with a time-reversal version of that of the variational system with zero initial state. The variational symmetry provides the following relation: for all $u_a \in L_2^m[t^0, t^1]$,

$$(\delta\Sigma^{x(t^0)}(u))^*(u_a) = \mathcal{R} \circ (\delta\Sigma^{\psi(t^0)}(w)) \circ \mathcal{R}(u_a), \tag{2}$$

where $\circ$ denotes the composition, and $w \in U$ and $\psi(t) \in X, t \in [t^0, t^1]$ satisfying

$$\mathcal{R}\left(\frac{\partial^2 H(x,u)}{\partial (x,u)^2}\right) = \left.\frac{\partial^2 H(x,u)}{\partial (x,u)^2}\right|_{\substack{x = \psi \\ u = w}}, \tag{3}$$

where $\mathcal{R}$ represents the time reversal operator on $[t^0, t^1]$ defined by

$$(\mathcal{R}(u))(t) = u(t^1 - t + t^0), \quad \forall t \in [t^0, t^1]. \tag{4}$$

From the relation (2), we convert an adjoint system to the corresponding variational one. Due to the linearity of the variational system, the difference approximation enables us to calculate the output of the variational system as

$$\begin{aligned}&\mathcal{R}\circ(\delta\Sigma^{\psi(t^0)}(w))\circ\mathcal{R}(u_a) \quad (5)\\&=\frac{1}{\epsilon}\mathcal{R}\circ(\Sigma^{\psi(t^0)}(w+\epsilon\mathcal{R}(u_a))-\Sigma^{\psi(t^0)}(w))+o(|\epsilon|),\end{aligned}$$

where $\lim_{|\epsilon|\to 0} o(|\epsilon|)/|\epsilon| = 0$. From Eqs. (2) and (5), the input-output mapping of the adjoint system can be obtained by only using the input-output data of the original system. This is a key technique of our learning framework based on the variational symmetry. The precise theorem is available in [8]. See also [20], for application to the optimal gait generation problem.

2.2 Iterative learning control using variational symmetry

We refer to the iterative learning control (ILC) of Hamiltonian systems based on variational symmetry in [8]. The objective of ILC is to find an optimal feedforward input and corresponding optimal trajectory which minimize a given cost function by iteration of laboratory experiments.

Consider the system $\Sigma^{x_{t^0}} : U \to Y$ in (1) and a cost function $\hat{\Gamma}(u, y) : U \times Y \to \mathbb{R}$. By utilizing the relation $y = \Sigma^{x_{t^0}}(u)$, the cost function can be written by $\Gamma(u) := \hat{\Gamma}(u, \Sigma^{x_{t^0}}(u)) : U \to \mathbb{R}$. Let us calculate the Fréchet derivative of the cost function in order to obtain the gradient with respect to the input u as follows:

$$\begin{aligned}(\delta\Gamma(u))(\delta u) &= \langle\partial_u\hat{\Gamma}(u,y),\delta u\rangle_U + \langle\partial_y\hat{\Gamma}(u,y),\delta y\rangle_Y\\&=\langle\partial_u\hat{\Gamma}(u,y)+(\delta\Sigma^{x_{t^0}}(u))^*(\partial_y\hat{\Gamma}(u,y)),\delta u\rangle_U\\&=:\langle\nabla\Gamma(u),\delta u\rangle_U. \quad (6)\end{aligned}$$

Well-known Riesz's representation theorem and the linearity of the Fréchet derivative guarantee that there exist functions $\partial_u\hat{\Gamma}(u,y)$ and $\partial_y\hat{\Gamma}(u,y)$ satisfying Eq. (6). Since $\nabla\Gamma(u)$ in Eq. (6) represents the gradient of the cost function with respect to u, the steepest descent method implies that one can reduce the cost function down at least to a local minimum by the following iteration law with a positive definite matrix $K_{(i)}$:

$$u_{(i+1)} = u_{(i)} - K_{(i)}\nabla\Gamma(u_{(i)}). \quad (7)$$

Here, the subscript (i) denotes the ith iteration in a laboratory experiment. However, calculation of the gradient $\nabla\Gamma(u)$ generally requires the precise knowledge of the plant system $\Sigma^{x_{t^0}}$ in calculating the output signal of the adjoint system corresponding to $(\delta\Sigma^{x_{t^0}}(u))^*(\partial_y\hat{\Gamma}(u,y))$. The variational symmetry of Hamiltonian systems enables one to avoid the problem. By using Eqs. (2) and (5), the iteration procedure with Eq. (7) can be executed by only input-output data of the plant system $\Sigma^{x_{t^0}}$, which is available from experiments.

3 Description of the plant system

Let us consider a fully actuated planar biped robot with knees and torso depicted in Fig. 1. The legs and the

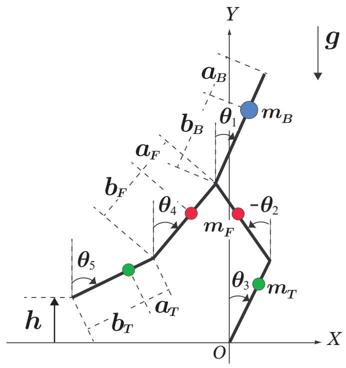

Fig. 1 Model of a planar kneed biped robot with a torso

torso are rigid bars, and they are connected by a frictionless hinge at each joint. A 1-period of walking describes the period between the take-off of one foot from the ground and its subsequent landing. Table 1 shows physical parameters. $\theta := (\theta_1, \theta_2, \theta_3, \theta_4, \theta_5)^\top$ represent

Table 1 Robot parameters

Notation	Meaning	Unit
m_B	Mass of the torso	kg
m_F	Mass of the femur	kg
m_T	Mass of the tibia	kg
l_B	Length of the torso	m
l_F	Length of the femur	m
l_T	Length of the tibia	m
b_B	Length from m_B to the hip joint	m
$a_B := l_B - b_B$		m
a_F	Length from the hip to m_F	m
$b_F := l_F - a_F$		m
b_T	Length from m_T to the toe	m
$a_T := l_T - b_T$		m
g	Gravity acceleration	m/s^2

the angles with respect to the vertical of the torso, the femur and the tibia of the stance leg, and those of the swing leg, respectively. $v := (v_1, v_2, v_3, v_4, v_5)^\top$ denote the torques relatively applied from the torso to the femur of the stance leg, from the femur to the tibia of the stance leg, from the tibia to the ground, from the torso to the femur of the swing leg, and from the the femur to the tibia of the swing leg, respectively. We impose the following assumptions on this robot.

Assumption 1 *The foot of the swing leg does not bounce back nor slip on the ground at the collision. That is, an inelastic impulsive impact is assumed.*

Assumption 2 *Transfer of support between the stance and the swing legs is instantaneous.*

We define the configuration coordinate as

$$q = (q_1, q_2, q_3, q_4, q_5)^\top := \theta,$$

and the control input u as

$$u = (u_1, u_2, u_3, u_4, u_5)^\top := Sv,$$
$$S = \begin{pmatrix} -1 & 0 & 0 & -1 & 0 \\ 1 & -1 & 0 & 0 & 0 \\ 0 & 1 & 1 & 0 & 0 \\ 0 & 0 & 0 & 1 & -1 \\ 0 & 0 & 0 & 0 & 1 \end{pmatrix} \tag{8}$$

in order to simplify the input-output relation in the Hamiltonian form. Then, the dynamics of this robot is described by a Hamiltonian system of the form (1) as

$$\begin{pmatrix} \dot q \\ \dot p \end{pmatrix} = \begin{pmatrix} 0_{5\times 5} & I_5 \\ -I_5 & 0_{5\times 5} \end{pmatrix} \begin{pmatrix} \frac{\partial H(q,p,u)}{\partial q}^\top \\ \frac{\partial H(q,p,u)}{\partial p}^\top \end{pmatrix},$$
$$\begin{pmatrix} q(t^0) \\ p(t^0) \end{pmatrix} = \begin{pmatrix} q_{t^0} \\ p_{t^0} \end{pmatrix}$$
$$y = -\frac{\partial H(q,p,u)}{\partial u}^\top = q \tag{9}$$

with the state $x = (q^\top, p^\top)^\top \in \mathbb{R}^{10}$ and the Hamiltonian

$$H(q,p,u) = \frac{1}{2} p^\top M(q)^{-1} p + U(q) - u^\top q. \tag{10}$$

Here, I_i and $0_{i\times j}$ represent the $i \times i$ identity and $i \times j$ zero matrices, respectively, and a symmetric positive definite matrix $M(q) \in \mathbb{R}^{5\times 5}$ denotes the inertia matrix. A scalar function $U(q) \in \mathbb{R}$ denotes the potential energy of the system. The generalized momentum $p \in \mathbb{R}^5$ is given by $p := M(q)\dot q$.

At the touchdown, a collision between the swing leg and the ground causes a discontinuous change in angular velocities. Assumptions 1 and 2 imply that there exists no double support phase. Since the support and swing legs change each other instantly, we have

$$q^+ = \begin{pmatrix} 1 & 0 & 0 & 0 & 0 \\ 0 & 0 & 0 & 1 & 0 \\ 0 & 0 & 0 & 0 & 1 \\ 0 & 1 & 0 & 0 & 0 \\ 0 & 0 & 1 & 0 & 0 \end{pmatrix} q^- =: Cq^-, \tag{11}$$

where q^- and q^+ denote the angles just before and just after the collision, respectively. Following the law of conservation of the angular momentum, a state transition mapping can be expressed by a matrix form as

$$\dot q^+ = \varPi(q^-)\dot q^- \tag{12}$$

with some matrix $\varPi(q^-)$ which depends only on q^-. For the detail of derivation of $\varPi(q^-)$, See, e.g., [25].

Before the ILC method mentioned in Subsection 2.2 is applied, a local feedback controller is typically employed to the control system in order to render the system asymptotically stable. It is known that in the case of a typical mechanical system as in (9), a simple PD feedback preserves the structure of the Hamiltonian system [7,8]. We consider the following local PD controller

$$u = -K_P q - K_D \dot q + \bar u\ , \tag{13}$$
$$K_P = \mathrm{diag}\{k_{p1}, k_{p2}, k_{p3}, k_{p4}, k_{p5}\},$$
$$K_D = \mathrm{diag}\{k_{d1}, k_{d2}, k_{d3}, k_{d4}, k_{d5}\},$$

where $\bar u$ is a new input for ILC and $K_P, K_D \in \mathbb{R}^{5\times 5}$ are chosen to be positive definite matrices. The resultant closed-loop Hamiltonian system is denoted by $\bar\varSigma(\bar u)$ as depicted in Fig. 2.

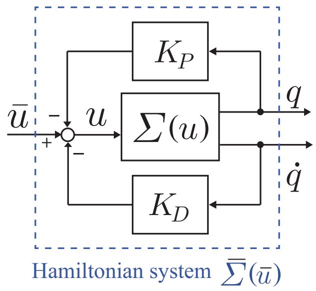

Fig. 2 Closed-loop Hamiltonian system $\bar\varSigma$ with the local PD controller

Remark 1 ([8]) Consider the feedback system of a typical mechanical system by a PD controller. If the inertia matrix $M(q)$ of the system does not depend on the configuration coordinate q, then we can let the conditions for the variational symmetry mentioned in Subsection 2.1 hold. Otherwise, however, if PD gains K_P and K_D are chosen large enough, we can still let the conditions satisfied approximately with arbitrary precision.

4 Main results

This section proposes an optimal gait generation method based on ILC mentioned in Section 2. In order to generate a 1-periodic walking trajectory, it is necessary that the state just after the collision should be equivalent to the initial state. However, the conventional ILC method in [8] does not deal with such discontinuous state transitions. Regarding this, we propose a learning framework, which can generate an optimal periodic trajectory taking discontinuous state transitions into account. We also provide a technique to avoid the foot-scuffing problem. First, we construct a desired terminal state corresponding to the state just before the collision, which will be transited to the initial state after the collision. Then, we derive the iteration law for learning so that the robot achieves the desired terminal state. However, the iteration law requires information of the Jacobian of the state transition mapping which maps from the velocity just before the collision to that just after the transition. Thus, second, we propose an estimation method of the Jacobian of the state transition mapping by the recursive least-squares, and incorporate it into the iteration law. Therefore, the proposed framework does not require the precise model of the robot nor the state transition mapping. Although the state transition mapping is often modeled by imposing the conservation law of the angular momentum, it does not strictly hold in practice. The proposed method can deal with the state transition mapping as a general nonlinear function.

4.1 Learning optimal gait generation method with state transition estimation

A proper reference trajectory for 1-periodic walking trajectory, denoted by y_d, is constructed by considering the effect of the discontinuous state transition. At the terminal time t^1, which corresponds to the time just before the collision, y_d has to satisfy $y_d(t^1) = Cy_{t^0}$ (the leg exchange matrix C is defined in Eq. (11)). Here, $y_{t^0} = y(t^0) = q_{t^0}$ represents a fixed initial value of the output generated by a fixed initial state x_{t^0} of the system (9). In what follows, we do not necessarily assume the model (12) under the conservation law of the angular momentum, but consider the model to be a general nonlinear function with respect to q^- and $\dot{q}^-$ instead, which is denoted as

$$\dot{q}^+ = f_\Pi(q^-, \dot{q}^-). \tag{14}$$

Note that $q^- = q(t^1) = y(t^1)$ holds between the configuration coordinate q and the system output y from the definition of the system (9). We impose the following assumption on the function f_Π.

Assumption 3 *By using the function f_Π in Eq. (14), define a mapping $f_\Pi^{q^-} : \mathbb{R}^m \to \mathbb{R}^m : \dot{q}^- \mapsto \dot{q}^+$ as*

$$f_\Pi^{q^-}(\cdot) := f_\Pi(q^-, \cdot).$$

Then, for any q^-, the mapping $f_\Pi^{q^-}$ is diffeomorphic.

In order to investigate the condition for the terminal velocity so that the state after the transition becomes equivalent to the initial state, we define the following inverse mapping of the transition $g_\Pi : \mathbb{R}^m \times \mathbb{R}^m \to \mathbb{R}^m : (q^+, \dot{q}^+) \mapsto \dot{q}^-$ as

$$g_\Pi(q^+, \dot{q}^+) := \left(f_\Pi^{Cq^+}\right)^{-1}(\dot{q}^+) = \dot{q}^-. \tag{15}$$

Then, the desired terminal coordinate and velocity for a 1-periodic trajectory, denoted by $(y_d^{-\top}, \dot{y}_d^{-\top})^\top$, should satisfy $\dot{y}_d^+ := f_\Pi(y_d^-, \dot{y}_d^-) = \dot{y}_{t^0}$ and $y_d^+ := Cy_d^- = y_{t^0}$. From the mapping g_Π in Eq. (15), the desired terminal velocity $\dot{y}_d^-$ is given by $\dot{y}_d^- = g_\Pi(y_{t^0}, \dot{y}_{t^0})$. Thus, we obtain the following reference trajectory, which is only valid around the terminal time t^1:

$$\begin{aligned} y_d(t) &:= \dot{y}_d^-(t - t^1) + Cy_{t^0} \\ &= g_\Pi(y_{t^0}, \dot{y}_{t^0})(t - t^1) + Cy_{t^0}. \end{aligned} \tag{16}$$

It is easily confirmed that the reference trajectory $y_d(t)$ satisfies the necessary conditions for a 1-periodic trajectory, that is, $y_d(t^1) = Cy(t^0)$ and $\mathrm{d}y_d(t^1)/\,\mathrm{d}t = \dot{y}_d^-$. As shown later, since the reference trajectory is only evaluated around the terminal time through a time filter function in the proposed iteration law, we simply define $y_d(t)$ as a linear function with respect to the time.

Second, we propose a constraint term for the cost function to be minimized in order to avoid the foot-scuffing problem. It attempts to lift the toe of the swing leg to a certain height around the middle time of the period, i.e., $(t^1 - t^0)/2$. As Fig. 1 illustrates, the height of the toe at the time t is given by

$$\begin{aligned} (h(y))(t) = l_F(\cos(y_2(t)) - \cos(y_4(t))) \\ + l_T(\cos(y_3(t)) - \cos(y_5(t))), \end{aligned} \tag{17}$$

where y_i denotes the ith element of y. We introduce a penalty function $F(h) \in \mathbb{R}$ with respect to the height, and two filter functions $\nu_1(t) \in \mathbb{R}$ and $\nu_2(t) \in \mathbb{R}$ with respect to the time. The penalty function is defined as

$$F(h) = \begin{cases} -\frac{1}{h_d^2}(h - h_d)^2(h + h_d) & (0 \le h \le h_d) \\ 0 & (h > h_d) \end{cases}, \tag{18}$$

where a design parameter $h_d \ge 0$ denotes the reference height. The filter functions are defined as

$$\nu_1(t) = \begin{cases} 0 & (t^0 \le t < t^1 - \Delta t) \\ \frac{1}{2}\left(1 - \cos\left(\frac{\Delta t - t^1 + t}{\Delta t}\pi\right)\right) & (t^1 - \Delta t \le t \le t^1) \end{cases} \tag{19}$$

$$\nu_2(t) = \begin{cases} \frac{1}{2}\left(1 - \cos\left(\frac{t^0 + t^1 - 2t}{2\Delta t}\pi\right)\right) & \left(\frac{t^0 + t^1 - 2\Delta\bar{t}}{2} \le t \le \frac{t^0 + t^1 + 2\Delta\bar{t}}{2}\right) \\ 0 & \left(t^0 \le t < \frac{t^0 + t^1 - 2\Delta\bar{t}}{2}, \frac{t^0 + t^1 + 2\Delta\bar{t}}{2} < t \le t^1\right), \end{cases} \tag{20}$$

where design parameters Δt and $\Delta\bar{t}$ denote positive constants. Fig. 3 illustrates $\nu_1(t)$ and $\nu_2(t)$.

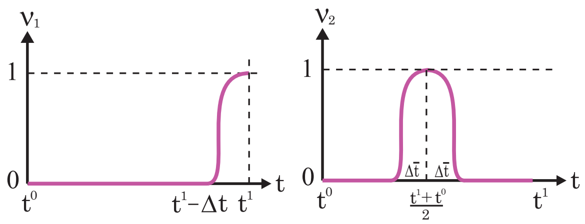

Fig. 3 Filter functions ν_1 and ν_2

Finally, we define the following cost function $\hat{\Gamma}(\bar{u}, y)$:

$$\hat{\Gamma}(\bar{u}, y) := \frac{1}{2}\int_{t^0}^{t^1} \Big((y(\tau) - y_d(\tau))^\top \nu_1(\tau) \Lambda_y (y(\tau) - y_d(\tau)) + \lambda_h \nu_2(\tau)(F(h(y(\tau))))^2 + \bar{u}(\tau)^\top \Lambda_{\bar{u}} \bar{u}(\tau)\Big)\, \mathrm{d}\tau. \tag{21}$$

Here, appropriate positive definite matrices $\Lambda_y, \Lambda_{\bar{u}} \in \mathbb{R}^{5\times 5}$ represent weight matrices for the constraint to make the trajectory periodic, and the input minimization, respectively. An appropriate positive constant λ_h represents a weighting coefficient for avoiding the foot scuffing problem.

In order to derive the iteration law for $\bar{u}$, the Fréchet derivative of the cost function (21) is calculated as

$$\begin{aligned}
\delta\hat{\Gamma}(\bar{u}, y)(\delta\bar{u}, \delta y) &= \langle \nu_1 \Lambda_y (y - y_d), \delta y\rangle \\
&\quad + \left\langle \lambda_h \nu_2 F(h(y)), \frac{\mathrm{d}F}{\mathrm{d}h}\frac{\partial h}{\partial y}\delta y \right\rangle + \langle \Lambda_{\bar{u}} \bar{u}, \delta\bar{u}\rangle \\
&= \left\langle \nu_1 \Lambda_y (y - y_d) + \lambda_h \nu_2 F(h(y)) \frac{\mathrm{d}F}{\mathrm{d}h}\frac{\partial h}{\partial y}^\top, \delta y \right\rangle \\
&\quad + \langle \Lambda_{\bar{u}} \bar{u}, \delta\bar{u}\rangle \\
&=: \langle \partial_y \hat{\Gamma}(\bar{u}, y), \delta y\rangle + \langle \partial_{\bar{u}} \hat{\Gamma}(\bar{u}, y), \delta\bar{u}\rangle \\
&= \langle \partial_{\bar{u}} \hat{\Gamma}(\bar{u}, y) + (\delta\bar{\Sigma}^{x_{t^0}}(\bar{u}))^* (\partial_y \hat{\Gamma}(\bar{u}, y)), \delta\bar{u}\rangle,
\end{aligned} \tag{22}$$

where $\partial_y \hat{\Gamma}(\bar{u}, y)$ and $\partial_{\bar{u}} \hat{\Gamma}(\bar{u}, y)$ denote the partial gradients of the cost function, respectively. It follows from Eqs. (17) and (18) that

$$\begin{aligned}
\frac{\partial h(y)}{\partial y} &= \\
&(0, -l_F \sin(y_2), -l_T \sin(y_3), l_F \sin(y_4), l_T \sin(y_5)) \\
\frac{\mathrm{d}F}{\mathrm{d}h} &= \begin{cases} -\frac{1}{h_d^2}(h - h_d)(3h + h_d) & (0 \le h \le h_d) \\ 0 & (h > h_d) \end{cases}.
\end{aligned} \tag{23}$$

From Eq. (22), the gradient of the cost function with respect to $\bar{u}$, denoted by $\nabla\Gamma(\bar{u})$, is given by

$$\begin{aligned}
&\nabla\Gamma(\bar{u}) = \\
&\partial_{\bar{u}} \hat{\Gamma}(\bar{u}, \bar{\Sigma}^{x_{t^0}}(\bar{u})) + (\delta\bar{\Sigma}^{x_{t^0}}(\bar{u}))^* (\partial_y \hat{\Gamma}(\bar{u}, \bar{\Sigma}^{x_{t^0}}(\bar{u}))).
\end{aligned} \tag{24}$$

From the iteration law for ILC in Eq. (7), the relation of the variational symmetry in Eq. (2) and the difference approximation in Eq. (5), the iteration law for the proposed learning method is derived as

$$\begin{aligned}
\bar{u}_{(i+1)} &= \bar{u}_{(i)} - K_{(i)} \partial_{\bar{u}} \hat{\Gamma}(\bar{u}_{(i)}, y_{(i)}) - \frac{K_{(i)}}{\epsilon_{(i)}} \\
&\times \mathcal{R}\left(\bar{\Sigma}^{\psi_{(i)}(t^0)}\left(\bar{w}_{(i)} + \epsilon_{(i)} \mathcal{R}(\partial_y \hat{\Gamma}(\bar{u}_{(i)}, y_{(i)}))\right)\right. \\
&\quad \left. - \bar{\Sigma}^{\psi_{(i)}(t^0)}(\bar{w}_{(i)})\right),
\end{aligned} \tag{25}$$

where $\epsilon_{(i)}$ denotes a sufficiently small positive constant, which is chosen to make the difference approximation (5) valid with the desired precision. For a given pair of the state $x = (q^\top, p^\top)^\top$ and the input $\bar{u}$, the literature [5] (see also [6]) gives a way to produce a pair of the initial condition $\psi(t^0)$ and the input $\bar{w}$ satisfying the condition in Eq. (3). The initial condition in the configuration and phase coordinates corresponding to $\psi_{(i)}(t^0)$, denoted by $Q^{\psi}_{t^0(i)}$, and $\bar{w}_{(i)}$ are given by

$$\begin{aligned}
Q^{\psi}_{t^0(i)} &= (y_{(i)}(t^1)^\top, -\dot{y}_{(i)}(t^1)^\top)^\top, \\
\bar{w}_{(i)} &= K_P \mathcal{R}(y_{(i)}) - K_D \mathcal{R}(\dot{y}_{(i)}).
\end{aligned} \tag{26}$$

Although the reference trajectory y_d in Eq. (16) is necessary to obtain the partial gradient $\partial_y \hat{\Gamma}(\bar{u}, y)$, calculation of the nonlinear mapping g_Π in Eq. (15) is required due to the desired velocity just before touchdown $\dot{y}_d^- = g_\Pi(y_{t^0}, \dot{y}_{t^0})$. We propose a technique to estimate $\dot{y}_d^-$ by the recursive least-squares with the stored experimental data. Since the following relation holds:

$$\mathrm{d}\dot{y}^- = \frac{\partial g_\Pi(y^+, \dot{y}^+)}{\partial(y^+, \dot{y}^+)} \begin{pmatrix} \mathrm{d}y^+ \\ \mathrm{d}\dot{y}^+ \end{pmatrix}, \tag{27}$$

we approximate $\mathrm{d}y^+, \mathrm{d}\dot{y}^+$ and $\mathrm{d}\dot{y}^-$ in Eq. (27) by differences between the desired coordinate and velocity just after the collision $(y_d^{+\top}, \dot{y}_d^{+\top})^\top$ and the stored data by the ith experiment. We define the estimate value of $\dot{y}_d^-$ at the ith iteration as

$$\widetilde{\dot{y}_d^-}_{(i)} := \dot{y}^-_{(i)} + \widetilde{\frac{\partial g_\Pi(y^+, \dot{y}^+)}{\partial(y^+, \dot{y}^+)}}\Bigg|_{\substack{y^+ = y_d^+ \\ \dot{y}^+ = \dot{y}_d^+}} \begin{pmatrix} y_d^+ - y^+_{(i)} \\ \dot{y}_d^+ - \dot{y}^+_{(i)} \end{pmatrix}. \tag{28}$$

We simultaneously calculate the estimations $\widetilde{\dot{y}_d^-}$ and $\widetilde{\partial g_\Pi}/\partial(y^+, \dot{y}^+)$ by the regularized recursive least-squares with a forgetting factor. We transform Eq. (28) using the relations $y_d^+ = y_{t^0}$ and $\dot{y}_d^+ = \dot{y}_{t^0}$ into

$$\dot{y}^-_{(i)} = \left(\widetilde{\frac{\partial g_\Pi(y^+, \dot{y}^+)}{\partial(y^+, \dot{y}^+)}}, \ \widetilde{\dot{y}_d^-}_{(i)}\right) \begin{pmatrix} y^+_{(i)} - y_{t^0} \\ \dot{y}^+_{(i)} - \dot{y}_{t^0} \\ 1 \end{pmatrix}. \tag{29}$$

For notational simplicity, we describe the relation (29) as $Y_{(i)} = \Phi X_{(i)}$ hereafter. We define the following cost function for the regularized least-squares with a forgetting factor:

$$\sum_{k=1}^{i}\rho^{i-k}(Y_{(k)}-\Phi X_{(k)})^\top(Y_{(k)}-\Phi X_{(k)})+\alpha\,\mathrm{tr}\{\Phi\Phi^\top\},$$

where ρ $(0<\rho\le 1)$ represents a constant forgetting factor. Then, from [3], the recursive formula is given by

$$W_{(i)}=\rho W_{(i-1)}+X_{(i)}X_{(i)}^\top, \qquad (30)$$
$$\Phi_{(i)}=\Phi_{(i-1)}+\left(Y_{(i)}-\Phi_{(i-1)}X_{(i)}\right)X_{(i)}{}^\top\left(W_{(i)}+\alpha I_{11}\right)^{-1}$$

with initial conditions $W_{(0)}=0_{11\times 11}$ and $\Phi_{(0)}=0_{5\times 11}$. From Eqs. (29) and (30), we can obtain the ith estimations as

$$\left(\frac{\partial \widetilde{g_\Pi(y^+,\dot y^+)}}{\partial(y^+,\dot y^+)},\widetilde{\dot y_d^-}_{(i)}\right)=\Phi_{(i)}. \qquad (31)$$

Consequently, from Eqs. (16) and (31), the reference trajectory $y_d(t)$ involved in the partial gradient $\partial_y\hat\Gamma(\bar u,y)$ in Eq. (25) can be estimated as

$$\widetilde{y_{d(i)}}=\widetilde{\dot y_d^-}_{(i)}(t-t^1)+Cy_{t^0} \qquad (32)$$

Let us summarize the proposed learning algorithm.

Step 0 : Set the total learning steps N, and appropriately positive definite matrices Λ_y and $\Lambda_{\bar u}$ and positive constant λ_h as weighting parameters, positive constants Δt, $\Delta\bar t$ and h_d as design parameters, positive definite matrices K_P and K_D in (13) and an initial condition $Q_{t^0}=(q_{t^0}^\top,\dot q_{t^0}^\top)^\top$. Choose the forgetting factor ρ satisfying $0<\rho\le 1$, and the regularization factor $\alpha>0$ for the recursive least-squares (30). Set $i=1$ and go to Step 1.

Step 1: Execute laboratory experiment with the initial condition Q_{t^0} and zero control input (or an appropriate initial input). Let $\bar u_{(i)}$ and $y_{(i)}$ be the input and the output data obtained by the ith experiment, respectively. Let $Y_{(1)}=\dot y^-_{(1)}$ and $X_{(1)}=\left(y_{(1)}^{+\top}-y_{t^0}^\top,\dot y_{(1)}^{+\top}-\dot y_{t^0}^\top,1\right)^\top$, and solve $\Phi_{(1)}$ via (30). Then, obtain $\widetilde{y_{d(1)}}$ from Eqs. (31) and (32). Set $k=1$. Then, go to Step $3k-1$.

Step $3k-1$: Execute the $(3k-1)$th laboratory experiment via the following iteration law:

$$\begin{cases}Q_{t^0(3k-1)}=(q(t^1)_{(3k-2)}^\top,-\dot q(t^1)_{(3k-2)}^\top)^\top\\ \bar u_{(3k-1)}=K_P\mathcal{R}(y_{(3k-2)})-K_D\mathcal{R}(\dot y_{(3k-2)})\end{cases}. \qquad (33)$$

Then, go to Step $3k$.

Step $3k$: Execute the $3k$th laboratory experiment via the following iteration law with a sufficiently small positive constant $\epsilon_{(k)}$

$$\begin{cases}Q_{t^0(3k)}=Q_{t^0(3k-1)}\\ \bar u_{(3k)}=\bar u_{(3k-1)}+\epsilon_{(k)}\mathcal{R}(\nu_1\Lambda_y(y_{(3k-2)}-\widetilde{y_{d(k)}})\\ \qquad +\lambda_h\nu_2F(h(y_{(3k-2)}))\frac{\mathrm{d}F}{\mathrm{d}h}\frac{\partial h}{\partial y}^\top)\end{cases}. \qquad (34)$$

Then, go to Step $3k+1$.

Step $3k+1$: Execute the $(3k+1)$th laboratory experiment via the following iteration law with an appropriate positive definite matrix $K_{(k)}$

$$\begin{cases}Q_{t^0(3k+1)}=Q_{t^0(3k-2)}\\ \bar u_{(3k+1)}=\bar u_{(3k-2)}-K_{(i)}\Big(\Lambda_{\bar u}\bar u_{(3k-2)}+\frac{1}{\epsilon_{(k)}}\\ \qquad \times\mathcal{R}(y_{(3k)}-y_{(3k-1)})\Big)\end{cases} \qquad (35)$$

Solve $\Phi_{(k+1)}$ via (30), and obtain $\widetilde{y_{d(k+1)}}$ from Eqs. (31) and (32).
If $k=N$, the learning procedure terminates. Otherwise, set $k=k+1$ and go to Step $3k-1$.

The 3-steps iteration laws imply that this learning procedure needs three experiments to execute a single update in (25). First, the $(3k-1)$th iteration generates a trajectory ψ by Eq. (26) with $x=x_{(3k-2)}$ so as to satisfy the condition (3) for using the variational symmetry (5). Second, in the $3k$th iteration, we calculate the output $\bar\Sigma^{\psi(t^0)}(\bar w+\epsilon\mathcal{R}(\partial_y\hat\Gamma))$ in Eq. (25) (note that in this case ψ corresponds to $x_{(3k-1)}$). Then, the input and the output signals of $(\delta\bar\Sigma^{x_{t^0}}(\bar u))^*(\partial_y\hat\Gamma)$ in Eq. (24) can be calculated from Eq. (25). With this information, the gradient of the cost function with respect to the input $\nabla\Gamma(\bar u)$ (see Eq. (24)) is obtained. Finally, the input for the $(3k+1)$th iteration is given by Eq. (25) with these signals.

Remark 2 A state trajectory under which the configuration coordinate q and the phase coordinate $\dot q$ satisfy

$$q(t)=q(t^1-t+t^0)$$
$$\dot q(t)=-\dot q(t^1-t+t^0),\qquad \forall t\in[t^0,t^1] \qquad (36)$$

is called a symmetric trajectory. When a state trajectory x with an input u is symmetric trajectory, the condition (3) is satisfied with $\psi=x$ and $w=u$. Then, if the learning procedure is executed around a symmetric trajectory, the procedure corresponding to the $(3k-1)$th iteration in (33) is not necessary. Thus, one can utilize the following 2-steps iteration laws instead of the 3-steps ones in (33), (34) and (35):

$$\begin{cases} Q_{t^0(2k)} = Q_{t^0(2k-1)} \\ \bar{u}_{(2k)} = \bar{u}_{(2k-1)} + \epsilon_{(k)} \mathcal{R}(\nu_1 \Lambda_y (y_{(2k-1)} - \widetilde{y_{d(k)}}) \\ \qquad + \lambda_h \nu_2 F(h(y_{(2k-1)})) \frac{\mathrm{d}F}{\mathrm{d}h} \frac{\partial h}{\partial y}^\top) \end{cases}, \quad (37)$$

$$\begin{cases} Q_{t^0(2k+1)} = Q_{t^0(2k-1)} \\ \bar{u}_{(2k+1)} = \bar{u}_{(2k-1)} - K_{(i)} \Big(\Lambda_{\bar{u}} \bar{u}_{(2k-1)} + \frac{1}{\epsilon_{(k)}} \\ \qquad \times \mathcal{R}(y_{(2k)} - y_{(2k-1)}) \Big) \end{cases}. \quad (38)$$

5 Numerical example

We apply the proposed algorithm in the previous section to the kneed biped with torso depicted in Fig. 1. The physical parameters of the robot are chosen as $m_B = 10.0$, $m_F = 3.0$, $m_T = 2.0$ kg, and $l_B = 0.70$, $a_B = 0.20$, $l_F = l_T = 0.50$, $a_F = a_T = 0.30$ m. Gains for the PD feedback (13) are selected as $k_{p1} = 20$, $k_{d1} = 15$, $k_{p2} = k_{p3} = k_{p4} = k_{p5} = 10$ and $k_{d2} = k_{d3} = k_{d4} = k_{d5} = 6$. We utilize the following design parameters with respect to the cost function (21) as $h_d = 5.0 \times 10^{-2}$m and $\Lambda_y = 30 I_5$, $\Lambda_{\bar{u}} = 1 \times 10^{-6} I_5$, $\lambda_h = 10$, those with respect to the filter functions ν_1 in Eq. (19) and ν_2 in Eq. (20) as $\Delta t = 8.0 \times 10^{-2}$, $\Delta \bar{t} = 0.30$ s, and those with respect to the learning algorithm as $\rho = 0.999$, $\alpha = 2$, $K_{(\cdot)} = 5 I_5$ and $\epsilon_{(\cdot)} = 1$, respectively. Although those parameters are empirically determined, we observed that some different pairs of the parameters also generate other walking gaits. Here, we show the results of applying the 2-steps iteration laws in Remark 2. We proceed 5000 steps of the learning procedure with the following initial condition:

$$q_{t^0} = (0.0, -0.12, 0.12, -0.12, -0.12),$$
$$\dot{q}_{t^0} = (0.0, 2.5, 0.1, 4.5, -2.5), \quad (39)$$

which is empirically determined.

Figure 4 shows the history of the cost function (21) along the iteration decreasing monotonically. It implies that optimization is executed smoothly. Figure 5 shows the estimation results of $||\widetilde{\dot{y}_d^-}_{(i)} - \dot{y}_d^-||$ by the recursive formula (30). Since Fig. 5 is only verification of the estimation, the true value $\dot{y}_d^-$ is not utilized in the learning procedure at all. From Figs. 4 and 5, both trajectory learning and estimation of the discontinuous velocity transition are achieved. The left figure in Fig. 6 represents the stick diagrams of the robot at the initial and terminal times before learning, namely, the autonomous motion from the initial condition (39). On the contrary, the right figure represents those after learning, namely, the resultant optimal gait. Those figures imply that a walking motion seems to be generated eventually. We also confirm that the resultant gait achieves proper foot clearance.

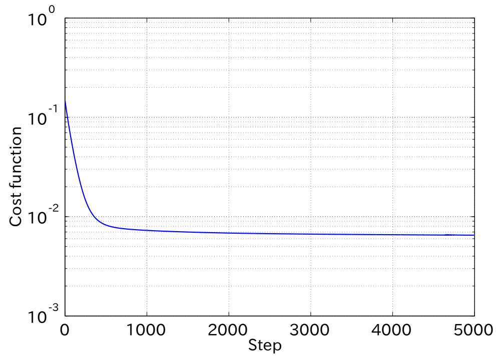

Fig. 4 Cost function

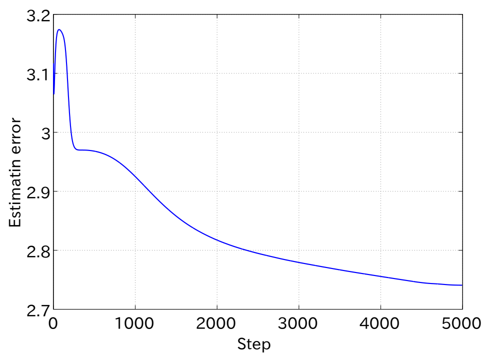

Fig. 5 Estimation error $||\widetilde{\dot{y}_d^-} - \dot{y}_d^-||$

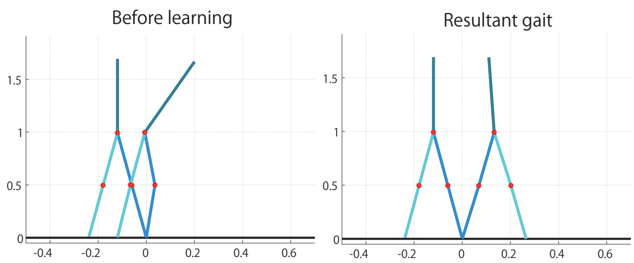

Fig. 6 Stick diagrams at the initial and terminal times before learning (Left) and after learning (Right)

6 Conclusion

In this paper, we have proposed a modification of our previous learning gait generation method by equipping a reference trajectory considering discontinuous velocity transitions properly. This method can generate an optimal feedforward control input and the corresponding periodic trajectory minimizing the L_2 norm of the control input. Although calculation of such reference trajectory generally requires information of the transition mapping, the proposed method estimates the mapping by the least-squares with the stored experimental data. Thus, it does not require the precise knowledge of the plant system nor the discontinuous state transition model. We have also proposed a technique to generate an optimal gait not only being energy-efficient but also avoiding the foot-scuffing problem. Finally, numerical simulations of a kneed biped with torso have demonstrated the validity of the proposed method.

References

1. Asano, F.: A novel gait generation method independent of target settling-time adjustment for underactuated limit cycle walking. Multibody System Dynamics **37**(2), 227–244 (2016)
2. Asano, F., Luo, Z.W.: Energy-efficient and high-speed dynamic biped locomotion based on principle of parametric excitation. IEEE Trans. Robotics **24**(6), 1289–1301 (2008)
3. Benesty, J., Paleologu, C., Ciochină, S.: Regularization of the RLS algorithm. IEICE Trans. Fundamentals **E94-A**(8), 1628–1629 (2011)
4. Crouch, P.E., van der Schaft, A.J.: Variational and Hamiltonian Control Systems, *Lecture Notes on Control and Information Science*, vol. 101. Springer-Verlag, Berlin (1987)
5. Fujimoto, K., Horiuchi, T., Sugie, T.: Iterative learning optimal control of Hamiltonian systems based on variational symmetry. Trans. the Institute of Systems Control and Information Engineers **21**(1), 10–17 (2008). (in Japanese)
6. Fujimoto, K., Koyama, I.: Iterative feedback tuning for Hamiltonian systems. In: Proc. 17th IFAC World Congress, pp. 15,678–15,683 (2008)
7. Fujimoto, K., Sugie, T.: Canonical transformation and stabilization of generalized Hamiltonian systems. Systems & Control Letters **42**(3), 217–227 (2001)
8. Fujimoto, K., Sugie, T.: Iterative learning control of Hamiltonian systems: I/O based optimal control approach. IEEE Trans. Autom. Contr. **48**(10), 1756–1761 (2003)
9. Goswami, A., Espiau, B., Keramane, A.: Limit cycles in a passive compass gait biped and passivity-mimicking control laws. Autonomous Robots **4**(3), 273–286 (1997)
10. Goswami, A., Thuilot, B., Espiau, B.: Compass-like biped robot part i: Stability and bifurcation of passive gaits. INRIA Research Report (2996) (1996)
11. Hyon, S., Emura, T.: Symmetric walking control: Invariance and global stability. In: Proc. IEEE ICRA, pp. 1455–1462 (2005)
12. Kato, Y., Ikemata, Y., Sano, A., Hayashi, Y., Fujimoto, H.: A basic study for passive walking that added upper body by means of spring mechanism. In: Proc. 13th Int. Conf. Climbing and Walking Robots and the Support Technologies for Mobile Machines, pp. 753–760 (2010)
13. Kinugasa, T., Ito, T., Kitamura, H., Ando, K., Fujimoto, S., Yoshida, K., Iribe, M.: 3D dynamic biped walker with flat feet and ankle springs: Passive gait analysis and extension to active walking. J. Robotics and Mechatronics **27**(4), 444–452 (2015)
14. Maschke, B., van der Schaft, A.J.: Port-controlled Hamiltonian systems: modelling origins and system theoretic properties. In: Proc. 2nd IFAC Symp. Nonlinear Control Systems, pp. 282–288 (1992)
15. McGeer, T.: Passive dynamic walking. Int. J. Robotics Research **9**(2), 62–82 (1990)
16. Osuka, K., Kirihara, K.: Motion analysis and experiments of passive walking robot QUARTET II. In: Proc. IEEE Int. Conf. Robotics and Automation, pp. 3052–3056 (2000)
17. Sano, A., Ikemata, Y., Fujimoto, H.: Analysis of dynamics of passive walking from storage energy and supply rate. In: Proc. IEEE Int. Conf. Robotics and Automation, pp. 2478–2483 (2003)
18. Satoh, S., Fujimoto, K., Hyon, S.: Gait generation for passive running via iterative learning control. In: Proc. IEEE/RSJ Int. Conf. Intelligent Robots and Systems, pp. 5907–5912 (2006)
19. Satoh, S., Fujimoto, K., Hyon, S.: Biped gait generation via iterative learning control including discrete state transitions. In: Proc. 17th IFAC World Congress, pp. 1729–1734 (2008)
20. Satoh, S., Fujimoto, K., Hyon, S.: Gait generation via unified learning optimal control of Hamiltonian systems. Robotica **31**(5), 717–732 (2013)
21. Satoh, S., Fujimoto, K., Saeki, M.: Transition to an optimal periodic gait by simultaneous input and parameter optimization method of Hamiltonian systems. Artificial Life and Robotics **21**(3), 258–267 (2016)
22. Satoh, S., Ikeda, M., Fujimoto, K., Hayakawa, Y.: Modification of learning optimal gait generation method in considering discontinuous velocity transitions. In: Proc. SICE 2010 Annual Conf., pp. 2794–2799 (2010)
23. Spong, M.W.: Passivity based control of the compass gait biped. In: Proc. of IFAC World Congress, pp. 19–23 (1999)
24. Ura, D., Sugimoto, Y., Sueoka, Y., Osuka, K.: Asymptotic realization of desired control performance by body adaptation of passive dynamic walker. J. Robotics and Mechatronics **29**(3), 480–489 (2017)
25. Westervelt, E.R., Grizzle, J.W., Chevallereau, C., Choi, J.H., Morris, B.: Feedback Control of Dynamic Bipedal Robot Locomotion. CRC Press (2007)